

Dendrimer-Mediated Multivalent Binding for the Enhanced Capture of Tumor Cells**

Ja Hye Myung, Khyati A. Gajjar, Jelena Saric, David T. Eddington, and Seungpyo Hong*

Multivalent binding, the simultaneous binding of multiple ligands to multiple receptors, has played a central role in a number of pathological processes, including the attachment of viral, parasitic, mycoplasmal, and bacterial pathogens.^[1] These biological activities have been extensively investigated to promote targeting of specific cell types,^[2] and biological multivalent inhibitors have yielded significant increases in binding avidities by one to nine orders of magnitude.^[3] In particular, nanoscale poly(amidoamine) (PAMAM) dendrimers have been reported to be an excellent mediator for facilitated multivalent effect owing to their capability to preorganize/orient ligands and the easy deformability of the polymer chains.^[2a]

We hypothesized that the advantages of enhanced binding avidity through the dendrimer-mediated multivalent effect could significantly improve detection of human disease-related rare cells (< 0.1 % subpopulation), such as circulating tumor cells (CTCs) in peripheral blood. Given the extreme rareness of CTCs (as few as one out of a billion hematologic cells), a very sensitive, specific detection is obviously necessary to achieve clinically significant CTC detection. Many efforts to increase sensitivity of CTC devices have been reported, which are mostly based upon engineering, such as topographical modifications^[4] and chaotic mixer fluidics.^[5] Herein, we have investigated a new approach to exploit naturally occurring processes using nanotechnology, that is, biomimetic nanotechnology. To create a highly sensitive surface utilizing the multivalent effect, we have employed seventh-generation (G7) PAMAM dendrimers and the anti-epithelial cell adhesion molecule (aEpCAM), as illustrated in Figure 1. Note that aEpCAM is one of the most commonly used CTC capturing agents,^[4a,5a,6] as EpCAM is often expressed by CTCs but not by normal hematological cells.^[4b,7] G7 PAMAM dendrimers were chosen owing to their adequate size (8–10 nm in diameter) and number of

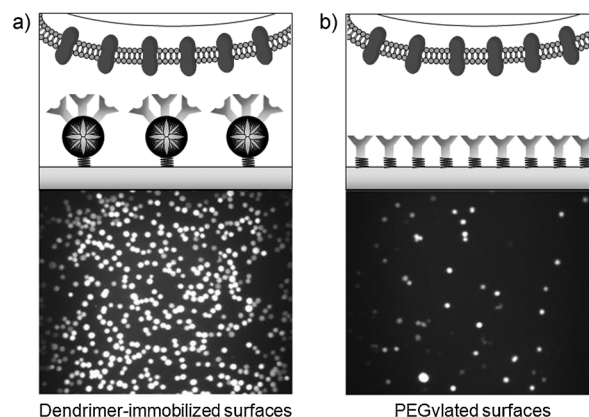


Figure 1. Illustration and fluorescence images of tumor cell capture on surfaces using aEpCAM immobilized with a) dendrimers and b) linear poly(ethylene glycol).

surface functional groups (512 theoretically) to accommodate multiple aEpCAM (around 5.5 nm in diameter of Fc region) per dendrimer, thereby enabling multivalent binding. Furthermore, another physiological process cell rolling mediated by E-selectin, mimicking the initial CTC recruiting process to the endothelium,^[8] has been also implemented to our device to further enhance surface sensitivity and specificity towards tumor cells.

To investigate the dendrimer-mediated multivalent binding, we directly measured the binding behaviors of the G7-aEpCAM conjugates using surface plasmon resonance (SPR).^[9] G7 PAMAM dendrimers were carboxylated and conjugated with aEpCAM, which was confirmed by ¹H NMR and size/zeta potential analyses (for details, see the Supporting Information).^[10] The UV analysis revealed that 2.8 and 4.9 aEpCAM molecules were conjugated per dendrimer, resulting in G7-(aEpCAM)_{2.8} and G7-(aEpCAM)_{4.9}, respectively. The binding parameters of the G7-aEpCAM conjugates to EpCAM-immobilized sensor chips were recorded and compared to those of free aEpCAM. The carboxylated G7 PAMAM dendrimers without aEpCAM showed no non-specific binding, assuring that the observed binding events of the G7-aEpCAM conjugates are the result of specific EpCAM-aEpCAM interactions. The SPR sensorgrams (Supporting Information, Figure S5) were used to obtain the quantitative binding kinetic parameters, such as association rate constant (k_a) and dissociation rate constant (k_d ; Table 1). Dissociation constants (K_D) were calculated from the measured k_a and k_d ($K_D = k_d/k_a = 1/K_A$), where a lower value of K_D corresponds to a stronger binding strength.

As listed in Table 1, the dendrimer conjugates show significantly lower K_D values than free aEpCAM. The

[*] J. H. Myung, K. A. Gajjar, J. Saric, Prof. D. T. Eddington, Prof. S. Hong
 Department of Biopharmaceutical Sciences, Department of Bioengineering, University of Illinois at Chicago
 833 South Wood St., Room 335, Chicago, IL, 60612 (USA)
 E-mail: sphong@uic.edu
 Homepage: <http://www.uic.edu/labs/honglab/index.html>

[**] This work was supported by the National Science Foundation (NSF) under grant no. CBET-0931472. This investigation was conducted in a facility constructed with support from the NCRR, NIH (grant C06RR15482). This research was also partially supported by the NCI, NIH (U54 CA151880), and the Chicago Biomedical Consortium.

Supporting information for this article is available on the WWW under <http://dx.doi.org/10.1002/anie.201105508>.

Table 1: Kinetic parameters for the binding of free aEpCAM and G7-aEpCAM conjugates to EpCAM measured by SPR.^[a]

	k_a [L mol ⁻¹ s ⁻¹]	k_d [s ⁻¹]	K_A [L mol ⁻¹]	K_D [mol L ⁻¹]	β
free aEpCAM	131	1.0×10^{-4}	1.4×10^6	7.3×10^{-7}	–
G7-(aEpCAM) _{2.8}	5.2×10^4	1.3×10^{-4}	2.8×10^8	3.5×10^{-8}	21.0
G7-(aEpCAM) _{4.9}	1.2×10^5	7.3×10^{-8}	1.8×10^{12}	5.8×10^{-13}	1.3×10^6

[a] All kinetic values were obtained by averaging at least three independent runs of SPR measurements. β = multivalency parameter.

changes in the dissociation constants can be expressed by the multivalency parameter β [Equation (1)]:^[1b,2a]

$$\beta K_N^{\text{multi}} = K^{\text{mono}} \quad (1)$$

where K^{mono} is the dissociation constant of free aEpCAM ($K^{\text{mono}} = 7.3 \times 10^{-7} \text{ mol L}^{-1}$), and N is the number of ligands (2.8 and 4.9) per dendrimer. The dissociation constants of the conjugates with multiple aEpCAMs, K_N^{multi} , were measured to be $K_{2.8}^{\text{multi}} = 3.5 \times 10^{-8} \text{ mol L}^{-1}$ and $K_{4.9}^{\text{multi}} = 5.8 \times 10^{-13} \text{ mol L}^{-1}$, providing β values of 21.01 and 1.26×10^6 , respectively. The phenomenal increase in binding avidity of G7-(aEpCAM)_{4.9} by a factor of approximately one million is largely due to the exponential decrease in k_d , which is typical for multivalent binding.^[2a]

To translate the multivalent binding benefit to enhanced tumor cell capture on surfaces, aEpCAM was covalently immobilized to G7 PAMAM dendrimer-coated surfaces and using a similar method described earlier (for details, see the Supporting Information).^[11] The cell adhesion of the dendrimer surfaces was compared to that of the linear polymer poly(ethylene glycol) (PEG)-immobilized (PEGylated) surfaces. Three breast cancer cell lines, MDA-MB-361, MCF-7, and MDA-MB-231 cells, were employed as CTC models. The comparison analysis using the cancer cells (Figure 2a) showed that the dendrimer-immobilized surfaces induced substantially more cells to be bound than the PEGylated surfaces for all three cell lines. The cell-bound surfaces were then agitated to show the stability of the cell binding on each surface. The number of remaining cells was normalized based on the initial cell number attached to each surface before agitation. Figure 2b shows that greater numbers of the bound cancer cells (MDA-MB-361 cells) remained on the dendrimer-immobilized surface upon agitation than those on the PEGylated

surface (for results using other cell lines, see the Supporting Information). To quantitatively analyze the multivalent effect in the cell adhesion experiments, the dissociation rate constant of the cell-surface complexes were calculated by non-linear curve fitting using the following exponential dissociation Equation (2):^[12]

$$Y = Y_p + A e^{-(kd)t} \quad (2)$$

where Y is the number of remaining cells on a surface at t , Y_p is the number of the surface-bound cells after reaching a

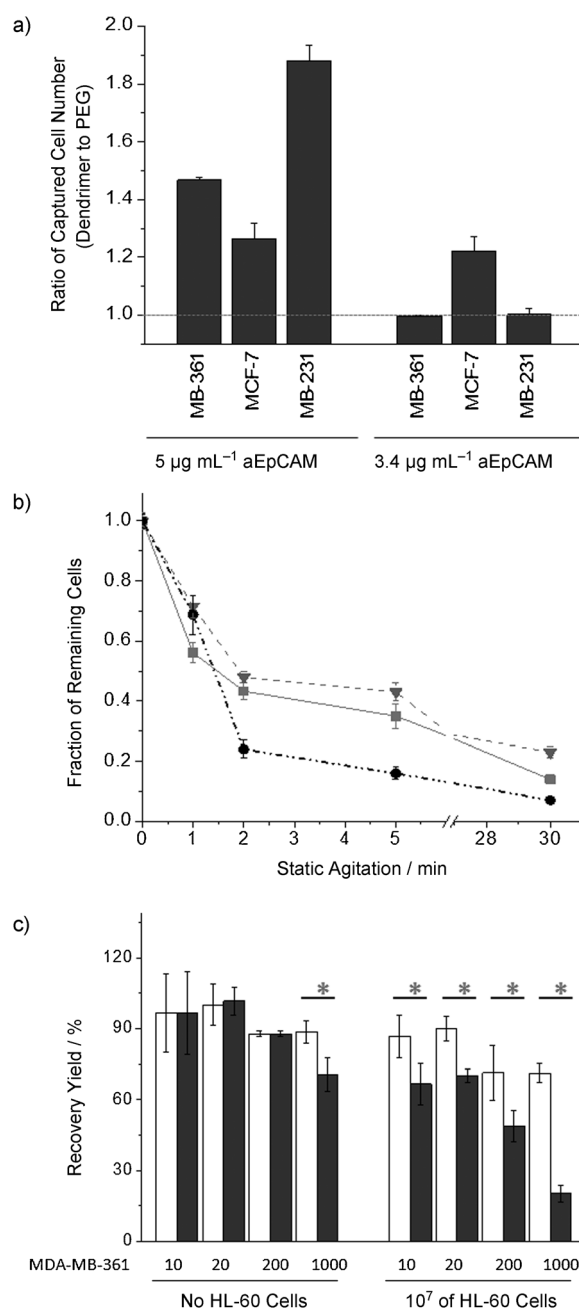


Figure 2. Enhanced cell adhesion and binding stability on dendrimer-coated surfaces under static conditions. a) Ratios of the numbers of the bound cancer cells on dendrimer-immobilized surfaces to those on the PEGylated surfaces. Error bars: standard error ($n > 3$). b) Dissociation kinetics of MDA-MB-361 cells on dendrimer-immobilized surfaces and PEGylated surfaces. ■ 5 µg mL⁻¹ aEpCAM on G7, ▼ 3.4 µg mL⁻¹ aEpCAM on G7, ● 5 µg mL⁻¹ aEpCAM on PEG. Error bars: standard error ($n = 3$). c) Recovery yields of captured MDA-MB-361 cells using various numbers (10, 20, 200, and 1000) of cells spiked with and without HL-60 cells. Significant improvements of the dendrimer surfaces were observed when either 10^3 of cancer cells were applied or the cells were mixed with HL-60 cells (10^7 cells per surface). Open bars = dendrimers, filled bars = PEG. Error bars: standard error ($n = 3$). Asterisks indicate $p < 0.05$.

plateau, A is the difference between the number of cells at 0 min and at the plateau, and t is time. The plateau is defined as the region where no more cells are being detached from the surfaces. Although the dissociation rate constants vary between the cell types, it is obvious that all cancer cells exhibit the significantly slower dissociation rates (up to 5.2-fold for MCF-7 cells) from the dendrimer-immobilized surfaces than those from the PEGylated surfaces (Supporting Information, Table S3). Association rates were also calculated using an equation published by Motulsky et al. (for details, see the Supporting Information).^[13] The dendrimer-immobilized surfaces induce the slow dissociation and the enhanced association of the cancer cells.

We also observed that dendrimer-coated surfaces accommodate more aEpCAM to be immobilized than the PEGylated surfaces do, even under identical protein immobilization conditions. This is an additional advantage of using dendrimers. However, it is possible that the observed enhancement in tumor cell capturing is simply due to the increased amount of aEpCAM present on the dendrimer-coated surfaces rather than the multivalent binding. To investigate this, a reduced concentration (from 5.0 to 3.4 $\mu\text{g mL}^{-1}$) of aEpCAM was applied onto the dendrimer-immobilized surfaces to match the surface density of aEpCAM on the PEGylated surfaces where 5.0 $\mu\text{g mL}^{-1}$ of aEpCAM was added (for details, see the Supporting Information). Although the number of the captured cells on the dendrimer-coated surfaces was reduced, the dendrimer-coated surfaces still exhibit similar or higher initial capture efficiencies than the PEGylated surface (Figure 2a, the right three bars). More importantly, the dendrimer surfaces show markedly decreased dissociation rate constants of the surface binding of the tumor cells (up to 3.6-fold) and the enhanced binding stability upon agitation (up to 15.2-fold), compared to the PEGylated surface counterparts (for details, see the Supporting Information). These results indicate that the multivalent binding effect mediated by dendrimers is the major factor that enhances the cancer cell capture efficiency and the surface binding strength of the tumor cells.

To further evaluate the tumor cell adhesion under various conditions, we performed a series of regression assays using Calcein AM-labeled MDA-MB-361 cells spiked with 10^7 HL-60 cells (Figure 2c). Human leukemia HL-60 cells were used as a control leukocyte model, and the numbers of the spiked cancer cells and HL-60 cells in the mixtures were decided to simulate the clinical samples (roughly 1 CTC per 10^3 – 10^6 leukocytes^[14]). Although the recovery yield (the number of the cells being captured divided by the number of the cells that were originally spiked) of the both surfaces was generally decreased with an increase in the number of the applied cells, the recovery yield of the dendrimer-immobilized surfaces (at least over 70 % regardless of the presence of HL-60 cells) was remarkably greater than those on the PEGylated surfaces. In contrast, the recovery yield of the PEGylated surfaces dropped rapidly from about 80 % to about 20 % when the cell mixtures were applied. These results further support that the dendrimer-immobilized surfaces are superior to the linear polymer-functionalized surfaces in terms of the detection sensitivity from the cell mixtures.

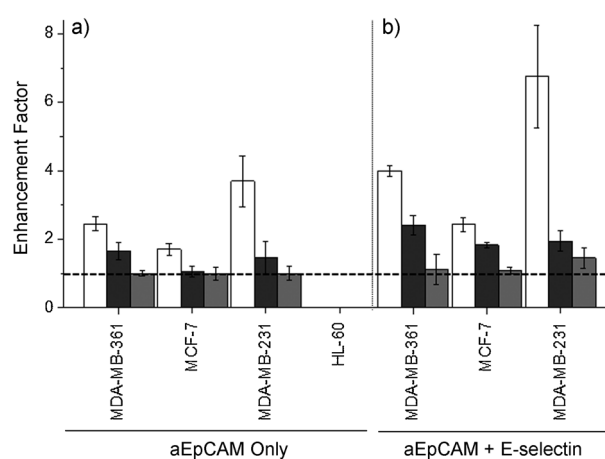


Figure 3. Enhanced cell binding stability by a combination of multivalent binding and cell rolling under flow. Three substrates (gray = epoxy-functionalized, black = PEGylated, and white = dendrimer-immobilized surfaces) treated with aEpCAM alone (a) or with both aEpCAM and E-selectin (b) were compared in terms of capture efficiency. The captured cancer cells on the surfaces were counted after injection of cell suspensions and washing with PBS at a shear stress of 0.8 dyn cm^{-2} , followed by normalization based on the number of each cell line on the epoxy-functionalized surfaces without E-selectin. An up to sevenfold enhancement in the capture efficiency by the dendrimer-immobilized surface was achieved through combination of rolling (E-selectin) and multivalent binding (aEpCAM). Error bars: standard error ($n=3$).

The dendrimer-mediated cell capture was further assessed under dynamic conditions (under flow) by comparing three substrates (epoxy functionalized, PEGylated, and dendrimer-immobilized) using a parallel-plate flow chamber.^[8a] Figure 3a shows fold enhancements in capture efficiency of the three surfaces after a harsh washing step (washing with PBS for 5 min at a flow rate of 500 $\mu\text{L min}^{-1}$ (0.8 dyn cm^{-2})). Compared to the epoxy-functionalized surface where aEpCAM was immobilized without a polymer linker (PEG or dendrimer), the PEGylated surface exhibited slightly improved capture efficiency (1.1–1.7-fold). More importantly, a significantly enhanced capture efficiency was observed on the surface with dendrimers (1.7–3.7-fold, Figure 3a), further supporting that dendrimers indeed mediated the multivalent binding effect in cell capture.

In our previous report, the biomimetic combination of dynamic rolling (E-selectin) and stationary binding (aEpCAM) showed substantially enhanced capture efficiency (more than threefold enhancement), as compared to a surface functionalized solely with aEpCAM.^[8a] To utilize the biomimetic effect, the three types of the aEpCAM-immobilized surfaces were treated with E-selectin and characterized by immunostaining using monoclonal anti-E-selectin-fluorescein (Supporting Information, Figure S9). The capture efficiencies of all three surfaces after addition of E-selectin were significantly improved than those treated only with aEpCAM (Figure 3), indicating that additional cell rolling mediated by E-selectin synergistically cooperates with stationary binding through aEpCAM. In particular, for the dendrimer-immobilized surface after adding E-selectin, a

remarkable seven-fold enhancement in capture efficiency was observed, as shown in Figure 3b in the case of MDA-MB-231 cells.

The dramatic enhancement in tumor cell capturing of the dendrimer surfaces is a result of the combined effect of multivalent binding and efficient protein immobilization, which is most likely due to the spherical architecture of dendrimers. Obviously, dendrimers can provide more functional groups available to protein immobilization than linear polymers. However, it is noteworthy to discuss why the same level of the multivalent binding was not observed in the linear polymer-coated surfaces. To induce the multivalent binding effect efficiently, the selection of scaffolds and linkers is crucial.^[15] The three-dimensional structure of the dendrimer organizes the ligands into a small region of space, as compared to what can be obtained when the ligands are conjugated to a linear polymer of similar molecular weight.^[2a,16] This geometric advantage likely reduces the energy of deformation (entropy) of ligands on the dendrimer surface to bind with their receptors, facilitating the localized multivalent binding. Furthermore, it has been known that the carboxylated dendrimer has good accessibility of target cells to the immobilized targeting ligands on the dendrimer surface,^[2c] and reduces denaturation of the ligands during immobilization.^[17]

Taken together, the significantly increased binding avidity of the G7-aEpCAM conjugates measured by SPR, along with the enhanced binding stability of the tumor cells on the dendrimer-functionalized surfaces, supports our hypothesis that the dendrimer-mediated multivalent binding effect can be exploited in cell capture on engineered surfaces. Additionally, we have shown that the combination of the two biomimetic approaches, that is, multivalent binding and cell rolling, substantially enhances the tumor cell detection. Our results demonstrate that the combination of nanotechnology and biomimicry has a great potential to be applied for highly sensitive detection of rare tumor cells from blood.

Received: August 3, 2011

Revised: September 8, 2011

Published online: October 25, 2011

Keywords: biomimetics · cell adhesion · dendrimers · multivalent binding · tumor cells

- [1] a) R. T. Lee, Y. C. Lee, *Glycoconjugate J.* **2000**, *17*, 543; b) M. Mammen, S. K. Choi, G. M. Whitesides, *Angew. Chem.* **1998**, *110*, 2908; *Angew. Chem. Int. Ed.* **1998**, *37*, 2754; c) M. Mourez, R. S. Kane, J. Mogridge, S. Metallo, P. Deschatelets, B. R. Sellman, G. M. Whitesides, R. J. Collier, *Nat. Biotechnol.* **2001**, *19*, 958.
- [2] a) S. Hong, P. R. Leroueil, I. J. Majoros, B. G. Orr, J. R. Baker, Jr., M. M. Banaszak Holl, *Chem. Biol.* **2007**, *14*, 107; b) L. L. Kiessling, N. L. Pohl, *Chem. Biol.* **1996**, *3*, 71; c) A. Quintana, E. Raczka, L. Piehler, I. Lee, A. Myc, I. Majoros, A. K. Patri, T. Thomas, J. Mule, J. R. Baker, Jr., *Pharm. Res.* **2002**, *19*, 1310; d) D. Peer, J. M. Karp, S. Hong, O. C. Farokhzad, R. Margalit, R. Langer, *Nat. Nanotechnol.* **2007**, *2*, 751; e) R. Weissleder, K. Kelly, E. Y. Sun, T. Shtatland, L. Josephson, *Nat. Biotechnol.* **2005**, *23*, 1418.
- [3] a) T. Christensen, D. M. Gooden, J. E. Kung, E. J. Toone, *J. Am. Chem. Soc.* **2003**, *125*, 7357; b) J. E. Gestwicki, C. W. Cairo, D. A. Mann, R. M. Owen, L. L. Kiessling, *Anal. Biochem.* **2002**, *305*, 149; c) P. I. Kitov, D. R. Bundle, *J. Am. Chem. Soc.* **2003**, *125*, 16271.
- [4] a) S. Nagrath, L. V. Sequist, S. Maheswaran, D. W. Bell, D. Irimia, L. Ulkus, M. R. Smith, E. L. Kwak, S. Digumarthy, A. Muzikansky, P. Ryan, U. J. Balis, R. G. Tompkins, D. A. Haber, M. Toner, *Nature* **2007**, *450*, 1235; b) S. Wang, H. Wang, J. Jiao, K. J. Chen, G. E. Owens, K. Kamei, J. Sun, D. J. Sherman, C. P. Behrenbruch, H. Wu, H. R. Tseng, *Angew. Chem.* **2009**, *121*, 9132; *Angew. Chem. Int. Ed.* **2009**, *48*, 8970.
- [5] a) S. L. Stott, C. H. Hsu, D. I. Tsukrov, M. Yu, D. T. Miyamoto, B. A. Waltman, S. M. Rothenberg, A. M. Shah, M. E. Smas, G. K. Korir, F. P. Floyd, Jr., A. J. Gilman, J. B. Lord, D. Winokur, S. Springer, D. Irimia, S. Nagrath, L. V. Sequist, R. J. Lee, K. J. Isselbacher, S. Maheswaran, D. A. Haber, M. Toner, *Proc. Natl. Acad. Sci. USA* **2010**, *107*, 18392; b) S. Wang, K. Liu, J. Liu, Z. T. Yu, X. Xu, L. Zhao, T. Lee, E. K. Lee, J. Reiss, Y. K. Lee, L. W. Chung, J. Huang, M. Rettig, D. Seligson, K. N. Duraiswamy, C. K. Shen, H. R. Tseng, *Angew. Chem.* **2011**, *123*, 3140; *Angew. Chem. Int. Ed.* **2011**, *50*, 3084.
- [6] W. He, H. Wang, L. C. Hartmann, J. X. Cheng, P. S. Low, *Proc. Natl. Acad. Sci. USA* **2007**, *104*, 11760.
- [7] a) F. Momburg, G. Moldenhauer, G. J. Hammerling, P. Moller, *Cancer Res.* **1987**, *47*, 2883; b) W. J. Allard, J. Matera, M. C. Miller, M. Repollet, M. C. Connelly, C. Rao, A. G. Tibbe, J. W. Uhr, L. W. Terstappen, *Clin. Cancer Res.* **2004**, *10*, 6897.
- [8] a) J. H. Myung, C. A. Launier, D. T. Eddington, S. Hong, *Langmuir* **2010**, *26*, 8589; b) C. J. Dimitroff, M. Lechpammer, D. Long-Woodward, J. L. Kutok, *Cancer Res.* **2004**, *64*, 5261.
- [9] J. H. Myung, K. A. Gajjar, R. M. Pearson, C. A. Launier, D. T. Eddington, S. Hong, *Anal. Chem.* **2011**, *83*, 1078.
- [10] a) S. Sunoqrot, J. W. Bae, S. E. Jin, R. M. Pearson, Y. Liu, S. Hong, *Bioconjugate Chem.* **2011**, *22*, 466; b) J. W. Bae, R. M. Pearson, N. Patra, S. Sunoqrot, L. Vukovic, P. Kral, S. Hong, *Chem. Commun.* **2011**, *47*, 10302.
- [11] S. Hong, D. Lee, H. Zhang, J. Q. Zhang, J. N. Resvick, A. Khademhosseini, M. R. King, R. Langer, J. M. Karp, *Langmuir* **2007**, *23*, 12261.
- [12] H. J. Motulsky, R. E. Brown, *BMC Bioinf.* **2006**, *7*, 123.
- [13] H. J. Motulsky, R. R. Neubig, *Curr. Protoc. Neurosci.* **2010**, chap. 7, Unit 7.5.
- [14] A. M. Sieuwerts, J. Kraan, J. Bolt-de Vries, P. van der Spoel, B. Mostert, J. W. Martens, J. W. Gratama, S. Sleijfer, J. A. Foekens, *Breast Cancer Res. Treat.* **2009**, *118*, 455.
- [15] T. Lindhorst in *Host-Guest Chemistry*, Vol. 218 (Ed.: S. Penadés), Springer, Berlin, **2002**, p. 201.
- [16] J. D. Reuter, A. Myc, M. M. Hayes, Z. Gan, R. Roy, D. Qin, R. Yin, L. T. Piehler, R. Esfand, D. A. Tomalia, J. R. Baker, Jr., *Bioconjugate Chem.* **1999**, *10*, 271.
- [17] P. K. Ajikumar, J. K. Ng, Y. C. Tang, J. Y. Lee, G. Stephanopoulos, H. P. Too, *Langmuir* **2007**, *23*, 5670.